TRENDS IN SCIENCES 2026; 23(9): 12909
https://doi.org/10.48048/tis.2026.12909 RESEARCH ARTICLE

Diversity of Bioactive Compounds from *Sphagnum junghuhnianum* and Their Antimicrobial Potential: An *In-Vitro* and *In-Silico* Assessment

Sinta R Pardosi, Etti Sartina Siregar* and Isnaini Nurwahyuni

Department of Biology, Faculty of Mathematics and Natural Sciences, Universitas Sumatera Utara, Medan 20155, Indonesia

(*Corresponding author's e-mail: etti1@usu.ac.id)

Received: 6 December 2025, Revised: 15 January 2026, Accepted: 22 January 2026, Published: 30 March 2026

Abstract

Sphagnum junghuhnianum is a moss species that has attracted attention as a potential natural source of antimicrobial agents. This study aimed to evaluate the antimicrobial activity of the methanolic extract of *S. junghuhnianum* and to explore its chemical profile using LC-HRMS combined with *in silico* approaches. Antimicrobial activity was assessed using disk diffusion assays against Gram-positive and Gram-negative bacteria, as well as pathogenic fungi. The extract exhibited notable antibacterial activity in preliminary screening, particularly against *Streptococcus pyogenes* (42.01 ± 0.33 mm) and *Staphylococcus aureus* (34.62 ± 2.21 mm), while no antifungal activity was observed under the tested conditions. LC-HRMS profiling revealed 514 putatively identified metabolites, of which 35 compounds were selected for further biological activity prediction and molecular docking analysis. PASS prediction suggested that several compounds may possess antimicrobial relevance. Molecular docking against Penicillin-Binding Protein 1 (PBP1) indicated that ursolic acid showed the most favorable binding affinity (−9.8 kcal/mol) compared to the reference ligand, suggesting a possible antibacterial mode of action. Overall, this study provides preliminary evidence supporting the antibacterial potential of *S. junghuhnianum* and highlights its relevance for future investigations involving quantitative bioassays and compound validation.

Keywords: Antimicrobial activity, Bioactive metabolites, Molecular docking, Penicillin-Binding Protein 1, *Sphagnum junghuhnianum*

Introduction

Bryophytes, particularly mosses belonging to the genus *Sphagnum*, represent an ecologically important plant group that plays a crucial role in maintaining ecosystem stability, especially in wetlands and humid forest environments. In addition to functioning as natural water reservoirs and long-term carbon sinks, *Sphagnum* species are known to produce a wide range of secondary metabolites that contribute to their ecological resilience. Previous studies have reported that *Sphagnum* contains diverse classes of bioactive compounds, including polysaccharides such as sphagnan, amino acids, carotenoids, fatty acids, triterpenes, sterols, and phenolic acids [1,2]. Identified phenolic acids include dihydroxybenzoic, gallic, vanillic, salicylic, caffeic, chlorogenic, *p*-coumaric, and cinnamic acids [3]. In addition, *Sphagnum* species contain unique flavonoids, including flavonols and flavanones, present in both aglycone and glycosylated forms [4]. The dominant phenolic compound, sphagnic acid, plays an important ecological role in peat formation by inhibiting microbial decomposition and lowering environmental pH [5,6], while sphagnan exhibits cation-exchange properties that influence nutrient retention in peatland ecosystems [7]. Several studies have further demonstrated that phenolics, flavonoids, and saponins in *Sphagnum* are associated with antimicrobial activity [8,9].

Sphagnum junghuhnianum is a moss species widely distributed in humid tropical regions, including Indonesia. Despite its ecological significance, studies

focusing on its chemical composition and biological properties remain limited. Previous investigations have reported that ethanol extracts of *S. junghuhnianum* exhibit antimicrobial activity against selected Gram-positive bacteria and fungi, suggesting the presence of secondary metabolites with potential antimicrobial relevance [10]. More recent studies have indicated that *S. junghuhnianum* exhibits biochemical activity related to enzyme production and secondary metabolite biosynthesis, further supporting its value as a subject for chemical and biological exploration [11]. However, comprehensive characterization of its metabolite profile remains scarce.

To date, no studies have examined the bioactive constituents of *S. junghuhnianum* from Indonesia, particularly from North Sumatra. Most existing research on *Sphagnum* species has focused primarily on taxonomy rather than microbiological or biochemical characterization. Given the growing threats to tropical forests caused by deforestation and other anthropogenic pressures, the investigation of bioactivity properties in *S. junghuhnianum* has become increasingly urgent and relevant.

Penicillin-Binding Protein 1 (PBP1) from *Staphylococcus aureus* is a key transpeptidase involved in the final stages of bacterial cell wall biosynthesis. The Protein Data Bank structure 7O4B provides detailed structural information on the enzyme's active site and its interaction with β-lactam antibiotics, which inhibit transpeptidase activity by acylating the catalytic serine residue [12]. This structural model has been widely used to investigate protein–ligand interactions and to explore mechanisms associated with β-lactam resistance in *S. aureus*, including methicillin-resistant strains (MRSA) [13]. Consequently, PBP1 represents a relevant molecular target for computational screening approaches aimed at identifying compounds with potential antibacterial relevance [14]. Natural secondary metabolites derived from mosses, including *S. junghuhnianum*, may possess structural features that enable interaction with this enzyme, although such interactions remain to be experimentally validated [15].

This study aims to investigate the metabolite profile of *Sphagnum junghuhnianum* using LC-HRMS and to evaluate its antimicrobial activity through preliminary *in vitro* screening. In addition, *in silico* approaches, including PASS prediction and molecular docking, were employed to explore the potential biological relevance of selected metabolites and their predicted interactions with bacterial protein targets. These computational analyses are intended to generate hypotheses and guide future experimental studies, rather than to establish definitive mechanisms or therapeutic applications. Overall, this work seeks to contribute to the growing body of knowledge on *Sphagnum*-derived metabolites and their possible relevance in antimicrobial research.

Materials and methods

Research materials and tools

Preparation of Sphagnum junghuhnianum extracts

A total of 2,000 g of *Sphagnum junghuhnianum* samples were collected from the Sicike-cike Nature Tourism Park, North Sumatra, Indonesia (coordinates: 2.652462°N, 380944°E). The samples were thoroughly rinsed with distilled water to remove soil particles and other impurities, then air-dried at room temperature for 7 - 10 days. The dried material was cut into small fragments and ground into a fine powder, yielding 100 g of dried sample. The powdered material (100 g) was placed into an Erlenmeyer flask and extracted with 3,000 mL of 70% methanol. The flask was sealed with plastic film and secured with a rubber band to prevent solvent evaporation. Maceration was carried out for 72 h at room temperature with occasional stirring. After extraction, the mixture was filtered, and the combined filtrates were concentrated under reduced pressure at 40 °C using a rotary evaporator, producing a viscous methanolic extract of *S. junghuhnianum*.

Figure 1 Population of *Sphagnum junghuhnianum* on the substrate.

Antibacterial assays of *Sphagnum junghuhnianum* extracts

Pathogens used for antibacterial activity

The antimicrobial activity of the extract was tested against selected pathogenic microorganisms, including Gram-positive and Gram-negative bacteria, as well as fungal strains. The test microorganisms included three Gram-positive bacteria: *Staphylococcus aureus* ATCC 25923, *Streptococcus pyogenes* ATCC 35041, and *Streptococcus mutans* ATCC 35668; and three Gram-negative bacteria: *Klebsiella pneumoniae* ATCC 700603, *Salmonella typhi* ATCC 14028, and *Porphyromonas gingivalis* ATCC 33277. In addition, two fungal strains were included, *Candida albicans* ATCC 32476 and *Aspergillus niger* ATCC 793772.

Antibacterial activity

The evaluation of antibacterial efficacy was conducted using the disc diffusion method [16]. Twenty mL of Mueller-Hinton Agar (MHA) medium was dispensed into sterile Petri dishes and allowed to solidify Bacterial suspensions were adjusted to the turbidity of a 0.5 McFarland standard and uniformly spread on the agar surface using sterile cotton swabs. Filter paper disks were impregnated with 100 µL methanolic extract of *S. Junghuhnianum* and placed onto the inoculated agar surface. Chloramphenicol served as the positive control, whereas DMSO was used as the negative control. Plates were incubated at room temperature for 24 h. After incubation, inhibition zone diameters were measured. Although Minimum Inhibitory Concentration (MIC) values were not determined in this study, the disk diffusion assay provided preliminary evidence of antibacterial activity. All antimicrobial assays were performed in triplicate, and the results are presented as mean ± standard deviation. Although minimum inhibitory concentration (MIC) values were not determined in this study, the disk diffusion assay provided preliminary qualitative evidence of antibacterial activity.

Antifungal and anti-candida activity

Antifungal assays were conducted using the disk diffusion method on Potato Dextrose Agar (PDA). A total of 20 mL of PDA medium was poured into Petri dishes and allowed to solidify. *Candida albicans* suspensions were standardized to the McFarland turbidity scale and spread evenly across the agar surface. Disks loaded with 100 µL of methanolic extract were placed onto the medium. Plates were incubated at room

temperature for 48 h. Following incubation, inhibition zones were measured to assess antifungal activity against *C. albicans* and *A. niger*.

Liquid Chromatography-high Resolution Mass Spectrometry (LC-HRMS) analysis

Metabolite profiling of *S. junghuhnianum* extract was performed using LC-HRMS. Compound separation was carried out using a Thermo Scientific™ Vanquish™ Horizon UHPLC system equipped with an Accucore™ Phenyl Hexyl column (100×2.1 mm^2, 2.6 µm). The mobile phase consisted of water with 0.1% formic acid (A) and acetonitrile with 0.1% formic acid (B), applied at a flow rate of 0.3 mL/min. A gradient elution from 5% to 90% B was performed over 25 min. Column temperature was maintained at 40 °C, and the injection volume was 5 µL. Detection was performed using a Thermo Scientific™ Orbitrap™ Exploris 240 HRMS in Full MS/dd-MS^2 mode under both positive and negative ionization modes. The mass resolution was set at 60,000 FWHM, with a scan range of 70 - 800 m/z and collision energies between 30 - 70 NCE. Ionization was conducted using a Heated Electrospray Ionization (H-ESI) source at spray voltages of 3,500 V (positive mode) and 2,500 V (negative mode), with a transfer tube temperature of 300 °C and a vaporizer temperature of 320 °C. For sample preparation, 50 mg of extract was dissolved in 1 mL of HPLC-grade methanol, vortexed for 1 min, sonicated for 30 min, centrifuged at 1,400×g for 5 min, and filtered through a 0.2 µm membrane prior to injection. Data acquisition and processing were carried out using Thermo Scientific™ Compound Discoverer 3.3 software with compound identification based on mzCloud, MassList Database, and ChemSpider libraries.

***In-silico* analysis**

Protein-ligan preparation

The bioactive compounds identified from *Sphagnum junghuhnianum* and used for this study are listed below along with their respective PubChem Compound Identifiers (CID): 4-(3-Dodecanyl)benzenesulfonic acid (CID: 29249), Gluconic acid (CID: 10690), 4-Methoxycinnamaldehyde (CID: 641294), Guttiferone E (CID: 5352088), Dilaurylmethylamine (CID: 76205), Ursolic acid (CID: 64945), 6-Gingerol (CID: 442793), Bilobetin (CID: 5315459), Xylarioic acid B (CID: 46832764), Brosimacutin C (CID: 10936790), Ceriporic acid C (CID: 9819908), Glycerophospho-N-palmitoyl ethanolamine (CID: 53393933), Garcinol (CID: 5490884), (−)-Desoxygambogenin (CID: 16078252), 3,4-Dihydroxyphenylacetic acid (CID: 547), 32-Hydroxy-ent-guttiferone M (CID: 139031624), Nootkatone (CID: 1268142), Questiomycin C (CID: 146682678), (+)-ar-Turmerone (CID: 160512), Polygodial (CID: 72503), Ginkgetin (CID: 139587180), Caerulomycin F (CID: 25192237), Momilactone (CID: 162644), 18β-Glycyrrhetinic acid (CID: 10114), Punctaporonin K (CID: 139584880), Aqabamycin A (CID: 46846125), Malyngolide dimer (CID: 46211780), Pulcherriminic acid (CID: 3083664), Mimosamycin (CID: 4198), Asperglaucide (CID: 10026486), Helquinoline (CID: 10466080), 5-O-Desosaminyl-6-O-methylerythronolide A (CID: 10579285), and Carbazomycin B (CID: 166449).

Prediction of biological activity using PASS online

The biological activities of the selected compounds were predicted using the Prediction of Activity Spectra for Substances (PASS) tool available on the Way2Drug server (http://way2drug.com/PassOnline/). The SMILES structures of each compound were obtained from PubChem (https://pubchem.ncbi.nlm.nih.gov) and submitted to the server for activity prediction. The results were interpreted based on the Pa (probability to be active) values, with the following criteria: $Pa > 0.70$ indicates high probability of exhibiting biological activity. $0.50 \leq Pa \leq 0.70$ indicates moderate to low probability of activity. $Pa < 0.50$: Low or negligible probability of activity. These predictions were used solely for hypothesis generation.

Prediction drug-likeness

Drug-likeness profiles of the compounds were evaluated using SwissADME (http://www.swissadme.ch/) according to Lipinski's Rule of 5, including molecular weight, hydrogen bond donors and acceptors, and lipophilicity. This evaluation was applied as an early-stage screening tool, not as confirmation of oral bioavailability.

Molecular docking analysis

The study employed Autodock Vina within PyRx 8.0.0 to perform docking analysis, treating the protein as the macromolecule and examining bioactive compounds and capivasertib as ligands. Docking utilized specific grid parameters centered at (1.3057×1.4901×0.3121) with dimensions (36.7569×19.5379×18.1727 Å). Visualization of the docking outcomes was accomplished using Discovery Studio 2024 software. The docking analysis was conducted as a supportive, hypothesis-generating approach to explore potential ligand-target interactions and does not constitute experimental confirmation of inhibitory activity.

Results and discussion

Antimicrobial activity of *Sphagnum junghuhnianum*

Based on **Table 1**, the methanolic extract of *Sphagnum junghuhnianum* exhibited antibacterial activity in disk diffusion screening against several pathogenic microorganisms, indicating its potential as a source of antibacterial agents. The largest inhibition zone was observed against *S. pyogenes* ATCC 35041 (42.01 ± 0.33 mm) (**Figure 2**), reflecting notable antibacterial activity under the tested conditions. This value was higher than the inhibition zones recorded for *S. aureus* ATCC 25923 (34.62 ± 2.21 mm) and *S. mutans* ATCC 65064 (11.53 ± 0.11 mm), suggesting differential susceptibility among Gram-positive bacteria. Although the antibacterial effect of the extract remained lower than that of the reference antibiotic chloramphenicol, the observed inhibition zones indicate that *S. junghuhnianum* contains secondary metabolites with potential antibacterial relevance. These findings are consistent with previous reports describing mosses as sources of bioactive compounds capable of inhibiting bacterial growth.

The comparatively lower inhibition observed against *S. mutans* suggests reduced susceptibility relative to other Gram-positive bacteria. This may be associated with intrinsic factors such as differences in cell wall architecture, biofilm-forming capacity, or other protective mechanisms that limit the effectiveness of certain antimicrobial compounds. Similar patterns have been reported previously, where extracts from moss species, including *S. junghuhnianum*, showed stronger antibacterial activity against selected Gram-positive bacteria than against other tested strains [17].

Among Gram-negative bacteria tested, inhibition was detected only against *P. gingivalis*, with inhibition zones of 9.03 ± 0.03 mm (50% extract) and 9.73 ± 0.51 mm (100% extract). No measurable inhibition was detected against *K. pneumoniae*, indicating limited antibacterial activity against Gram-negative bacteria overall. This observation is consistent with the known resistance mechanisms of Gram-negative bacteria, particularly the presence of an outer lipopolysaccharide membrane that restricts the penetration of many antimicrobial compounds [18].

In contrast, the methanolic extract did not exhibit any antifungal or anti-yeast activity. No inhibition was observed against *A. niger* or *C. albicans*, while the positive control (ketoconazole) produced clear inhibition zones of 10.22 ± 0.07 mm and 17.16 ± 0.05 mm, respectively. These results indicate that the active metabolites in *S. junghuhnianum* are likely bactericidal or bacteriostatic primarily targeting Gram-positive bacteria rather than broad-spectrum antimicrobial compounds

These findings are supported by [19], who demonstrated that moss-derived secondary metabolites such as phenolics, flavonoids, and tannins are closely associated with antimicrobial properties. Similarly, [20] reported that flavonoids inhibit bacterial growth through mechanisms such as membrane disruption, enzyme inhibition, and protein binding. Furthermore, the phenolic and flavonoid content of *S. junghuhnianum* has been shown to vary with ecological conditions such as altitude [21], suggesting that environmental factors at the collection site may influence antimicrobial potency.

Table 1 Antimicrobial activity of the methanolic extract of *Sphagnum junghuhnianum*.

Extract	Test microorganisms		Inhibition zone (mm)			Positive control
			25%	50%	100%	Chloramphenicol (1000 ppm)/Nystatin (10,000 mg/L)
Sphagnum junghuhnianum	Gram-negative bacteria	*Porphyromonas gingivalis* ATCC 33277	0	9.03 ± 0.03	9.73 ± 0.51	18.05 ± 0.41
		Klebsiella pneumoniae ATCC 700603	0	0	0	12.15 ± 0.68
		Salmonella typhi ATCC 14028	0	0	0	22.36 ± 0.84
	Gram-positive bacteria	*Streptococcus mutans* ATCC 65064	0	0	0	20.37 ± 0.59
		Streptococcus pyogenes ATCC 35041	0	11.98 ± 1.08	17.02 ± 2.58	42.01 ± 0.33
		Staphylococcus aureus ATCC 25923	0	8.96 ± 0.32	9.99 ± 0.71	34.62 ± 2.21
	Fungi	*Aspergillus niger* ATCC 793772	0	0	0	10.22 ± 0.07 (Nystatin)
	Yeast	*Candida albicans* ATCC 32476	0	0	0	17.16 ± 0.05 (Nystatin)

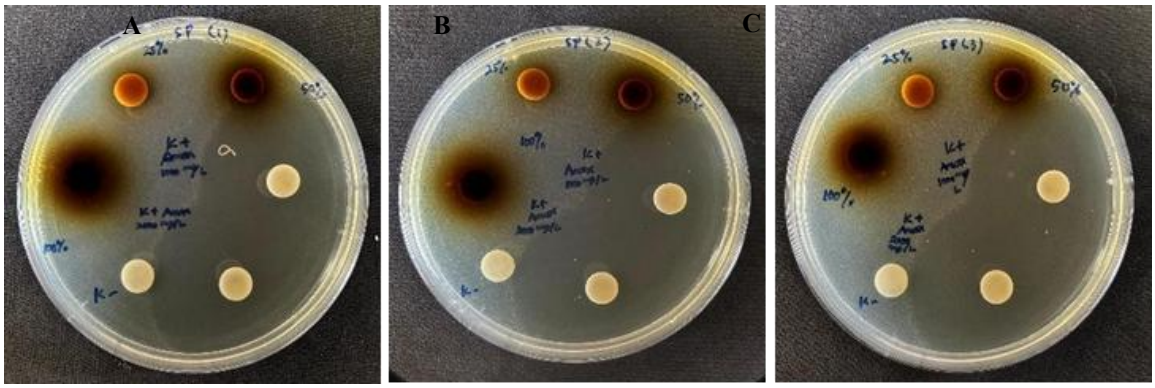

Figure 2 Inhibition zones of the methanolic extract of *Sphagnum junghuhnianum* against *S. pyogenes* ATCC 35041 (replicates 1, 2, and 3).

LC-HRMS Analysis

Bioactive compounds of Sphagnum junghuhnianum Dozy & Molk

LC-HRMS profiling of *S. junghuhnianum* Dozy & Molk revealed a total of 514 putatively annotated metabolites, indicating a high level of chemical diversity. To explore compounds with potential biological relevance, particularly those associated with antimicrobial-related activities, a targeted compound selection approach was applied. This selection was based on literature surveys and

database mining using KEGG, ChEBI, PubChem, and NPAtlas. Compounds previously reported to exhibit antibacterial, antifungal, or general antimicrobial activities were prioritized for further computational evaluation. A total of 35 compounds met the criteria and were selected for further *in silico* screening. Selection criteria included MS/MS fragmentation data, peak intensity (relative abundance), and association with known biosynthetic pathways of antimicrobial metabolites. The selected compounds include: 4-(3-Dodecanyl)benzenesulfonic acid (CID: 29249), Gluconic acid (CID: 10690), 4-Methoxycinnamaldehyde (CID: 641294), Guttiferone E (CID: 5352088), Dilaurylmethylamine (CID: 76205), Ursolic acid (CID: 64945), 6-Gingerol (CID: 442793), Bilobetin (CID: 5315459), Xylarioic acid B (CID: 46832764), Brosimacutin C (CID: 10936790), Ceriporic acid C (CID: 9819908), Glycerophospho-N-palmitoyl ethanolamine (CID: 53393933), Garcinol (CID: 5490884), (−)-Desoxygambogenin (CID: 16078252), 3,4-Dihydroxyphenylacetic acid (CID: 547), 32-Hydroxy-ent-guttiferone M (CID: 139031624), Nootkatone (CID: 1268142), Questiomycin C (CID: 146682678), (+)-ar-Turmerone (CID: 160512), Polygodial (CID: 72503), Ginkgetin (CID: 139587180), Caerulomycin F (CID: 25192237), Momilactone (CID: 162644), 18-β-Glycyrrhetinic acid (CID: 10114), Punctaporonin K (CID: 139584880), Aqabamycin A (CID: 46846125), Malyngolide dimer (CID: 46211780), Pulcherriminic acid (CID: 3083664), Mimosamycin (CID: 4198), Asperglaucide (CID: 10026486), Helquinoline (CID: 10466080), 5-O-Desosaminyl-6-O-methylerythronolide A (CID: 10579285), and Carbazomycin B (CID: 166449). Retention times for these compounds are presented in Table 2, while the chromatographic profile is shown in **Figure 3**.

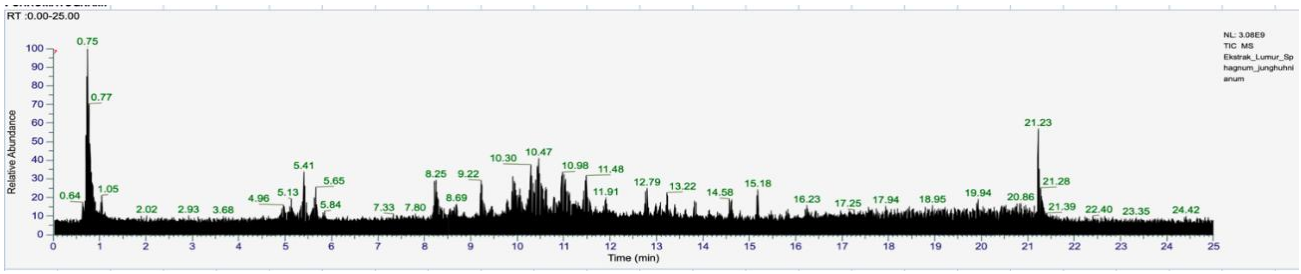

Figure 3 Chromatogram of LC-HRMS analysis of *Sphagnum junghuhnianum* Dozy & Molk.

Table 2 Identified compounds from *Sphagnum junghuhnianum* Dozy & Molk. based on LC-HRMS analysis.

Compound name	Mol. Formula	R. time (min)	Smiles	PubChem ID
4-(3-Dodecanyl) Benzenesulfonic Acid	C18H30O3S	10.613	CCCCCCCCCC(CC)C1=CC=C(C=C1)S(=O)(=O)O	29249
Gluconic Acid	C6 H12 O7	0.719	C(C(C(C(C(C(=O)O)O)O)O)O)O)O	10690
4-Methoxycinnamaldehyde	C10 H10 O2	11.697	COC1=CC=C(C=C1)/C=C/C=O	641294
Guttiferone E	C38 H50 O6	15.323	CC(=CCC1CC2(C(=O)C(=C(C3=CC(=C(C=C3)O)O)O)C(=O)C(C2=O)(C1(C)C)CC=C(C)C)CC(CC=C(C)C)C(=C)C)C	5352088
Dilaurylmethylamine	C25H53 N	14.929	CCCCCCCCCCCCN(C)CCCCCCCCCCCC	76205

Compound name	Mol. Formula	R. time (min)	Smiles	PubChem ID
Ursolic Acid	C30H48 O3	12.79	CC1CCC2(CCC3(C(=CCC4C3(CCC5C4(CCC(C5(C)C)O)C)C)C2C1C)C)C(=O)O	64945
6-Gingerol	C17H26O4	10.165	CCCCCC(O)CC(=O)CCc1ccc(O)c(OC)c1	442793
Bilobetin	C31H20O10	8.781	COC1=C(C=C(C=C1)C2=CC(=O)C3=C(C=C(C=C3O2)O)O)C4=C(C=C(C5=C4OC(=CC5=O)C6=CC=C(C=C6)O)O)O	5315459
Xylarioic acid B	C11H22O5	6.75	CCC(C)C(C(C)(C(C(C)C(=O)O)O)O)O	46832764
Brosimacutin C	C20H22O5	11.695	CC(C)(CCC1=C(C=CC2=C1OC(CC2=O)C3=CC=C(C=C3)O)O)O	10936790
Ceriporic acid C	C21H36 O4	1	CCCCCCCC/C=C\CCCCCCC(C(=C)C(=O)O)C(=O)O	9819908
Glycerophospho-N-palmitoyl ethanolamine	C21H44N7P	10.235	CCCCCCCCCCCCCCCC(=O)NCCOP(=O)(O)OCC(CO)O	53393933
Garcinol	C38 H50O6	14.17	C=C(C)C(CC=C(C)C)CC12CC(CC=C(C)C)C(C)(C)C(CC=C(C)C)(C(=O)C(=C(O)c3ccc(O)c(O)c3)C1=O)C2=O	5490884
(−)-Desoxygambogenin	C38 H48O6	13.907	CC(C)=CCCC(C)=CCc1c(O)c(CC=C(C)C)c2c(c1O)C(=O)C1=CC3CC4C(C)(C)OC(CC=C(C)C)(C3=O)C14O2	16078252
3,4-Dihydroxyphenylacetic acid	C8H8O4	7.814	C1=CC(=C(C=C1CC(=O)O)O)O	547
32-hydroxy-ent-guttiferone M	C38H50O7	13.055	CC(C)=CCC(O)C(C)=CCC12CC(CC=C(C)C)C(C)(C)C(CC=C(C)C)(C(=O)C(=C(O)c3ccc(O)c(O)c3)C1=O)C2=O	139031624
Nootkatone	C15H22O	10.785	C=C(C)C1CCC2=CC(=O)CC(C)C2(C)C1	1268142
Questiomycin C	C13H10N2OS	2.325	CS(=O)C1=C(C(=O)C=C2C1=NC3=CC=CC=C3O2)N	146682678
(+)-ar-Turmerone	C15H20O	9.762	CC(C)=CC(=O)CC(C)c1ccc(C)cc1	160512
Polygodial	C15H22O2	10.455	CC1(C)CCCC2(C)C(C=O)C(C=O)=CCC12	72503
Ginkgetin	C32H22O10	10.122	COC1=C(C=C(C=C1)C2=CC(=O)C3=C(C=C(C=C3O2)OC)O)C4=C(C=C(C5=C4OC(=CC5=O)C6=CC=C(C=C6)O)O)O	5271805

Compound name	Mol. Formula	R. time (min)	Smiles	PubChem ID
Thermolide G	C34H63NO9	12.29	CC(=O)OC(C(C)CC(C)C(O)C(C)C(C)O)C(C)CC(C)C1OC(=O)C(C(C)C)NC(=O)CC(O)CC(O)C(C)CC1C	139587180
Caerulomycin F	C12H12NO2	2.825	COC1=CC(=NC(=C1)C2=CC=CC=N2)CO	25192237
Momilactone	C20H26O3	10.425	C=CC1(C)CCC2C(=CC3OC(=O)C4(C)C(=O)CCC2(C)C34)C1	162644
18-β-Glycyrrhetinic acid	C30 H46O4	10.922	CC1(C(=O)O)CCC2(C)CCC3(C)C(=CC(=O)C4C5(C)CCC(O)C(C)(C)C5CCC43C)C2C1	10114
Punctaporonin K	C21H33NO5	10.307	C=C1CCC2(O)C(CC2(C)C)C(CO)=CC(O)C1NC(=O)C=C(C)CCO	139584880
Aqabamycin A	C16H11NO3	6.628	C1=CC=C(C=C1)C2=C(C(=O)NC2=O)C3=CC=C(C=C3)O	46846125
Farinomalein	C10 H13NO4	1.981	CC(C)C1=CC(=O)N(C1=O)CCC(=O)O	44254797
Malyngolide dimer	C32H60O6	15.272	CCCCCCCCCC1(CO)CCC(C)C(=O)OC(CO)(CCCCCCCCC)CCC(C)C(=O)O1	46211780
Pulcherriminic acid	C12H20N2O4	4.626	CC(C)CC1=C([N+](=C(C(=O)N1O)CC(C)C)[O-])O	3083664
Mimosamycin	C12H11NO4	2.805	CC1=C(C(=O)C2=CN(C(=O)C=C2C1=O)C)OC	4198
Asperglaucide	C27H28 N2O4	9.972	CC(=O)OCC(Cc1ccccc1)NC(=O)C(Cc1ccccc1)NC(=O)c1ccccc1	10026486
Helquinoline	C12H15NO3	1.938	COC1CC(C)Nc2c(C(=O)O)cccc21	10466080
5-O-Desosaminyl-6-O-methylerythronolide A	C30H55NO10	11.726	CCC1OC(=O)C(C)C(O)C(C)C(OC2OC(C)CC(N(C)C)C2O)C(C)(OC)CC(C)C(=O)C(C)C(O)C1(C)O	10579285
Carbazomycin B	C15 H15 N O2	8.988	CC1=C(C(=C(C2=C1NC3=CC=CC=C32)O)OC)C	166449

Prediction of compound biological activities

PASS Online prediction analysis (**Table 3**) was employed to provide a preliminary estimation of the potential biological activities of the compounds identified from *S. junghuhnianum*. The results indicated that several compounds were associated with predicted activities related to antimicrobial, antiviral, antiprotozoal, and enzyme-inhibitory functions, including activities linked to processes such as cell-wall biosynthesis [22]. A number of metabolites exhibited moderate to high Pa values, suggesting potential biological relevance within these activity categories. Compounds such as gluconic acid, 3,4-dihydroxyphenylacetic acid, thermolide G, 18-β-glycyrrhetinic acid, and farinomalein displayed predicted activity across multiple categories, indicating chemical diversity in their possible biological roles.

Among the analyzed compounds, 5-O-desosaminyl-6-O-methylerythronolide A showed relatively high Pa values in several predicted activity classes, including general anti-infective, anti-*Helicobacter pylori*, and antiprotozoal categories. While

these results suggest a broad predicted bioactivity profile, they should be interpreted cautiously, as PASS predictions do not confirm biological efficacy and require experimental validation.

Several other compounds, including ursolic acid, bilobetin, nootkatone, ginkgetin, and caerulomycin F, were predicted to possess antiprotozoal-related activities, particularly against *Leishmania* and *Trypanosoma*. These predictions may reflect possible interactions with protozoal cellular targets; however, specific mechanisms of action cannot be inferred solely from PASS analysis. In addition, a subset of compounds was predicted to be associated with enzyme-related activities, including glucan endo-1,3-β-D-glucosidase and peptidoglycan glycosyltransferase, which may be relevant to antimicrobial processes but remain speculative at this stage.

Predicted antiviral activities were also observed for several metabolites, particularly in categories associated with influenza viruses, rhinoviruses, and picornaviruses. Compounds such as 18-β-glycyrrhetinic acid, 6-gingerol, and brosimacutin C exhibited moderate to high Pa values in selected antiviral categories, suggesting potential relevance for further exploratory studies. In contrast, compounds including helquinoline, momilactone, and mimosamycin consistently showed low predicted activity scores and may therefore be considered lower-priority candidates for subsequent investigation.

Overall, the PASS prediction results indicate that a subset of the analyzed compounds may possess potential antimicrobial and anti-infective relevance, serving as a basis for hypothesis generation and compound prioritization. These computational predictions provide preliminary guidance for future experimental screening, but *in vitro* and *in vivo* validation will be essential to confirm the biological significance of the predicted activities.

Table 3 Prediction of the biological activity of compounds from *Sphagnum junghuhnianum* via the pass online test.

Compound name	Biological activity	Pa	Pi	Criteria
4-(3-Dodecanyl) Benzenesulfonic Acid	Antiseptic	0.787	0.004	High
	Membrane integrity antagonist	0.775	0.009	High
	Antiinfective	0.727	0.006	High
Gluconic Acid	Macrophage stimulant	0.914	0.001	Very high
	Membrane integrity agonist	0.926	0.005	Very high
	Levansucrase inhibitor	0.964	0.000	Very high
4-Methoxycinnamaldehyde	Membrane integrity agonist	0.833	0.028	Very high
	Polyporopepsin inhibitor	0.768	0.025	High
	Antiprotozoal (Leishmania)	0.502	0.024	High
Guttiferone E	Antibacterial	0.621	0.008	High
	Antiprotozoal (Trypanosoma)	0.591	0.009	High
	Antiviral (Rhinovirus)	0.488	0.029	Low
Dilaurylmethylamine	Antiviral (Poxvirus)	0.630	0.013	High
	Antiviral (Picornavirus)	0.547	0.033	High
	Antiviral (Adenovirus)	0.515	0.00	High
Ursolic Acid	Antiprotozoal (Leishmania)	0.915	0.003	Very high
	Antiviral (Influenza)	0.761	0.004	High
	Glucanendo-1,3-beta-D-glucosidase inhibitor	0.572	0.034	High
6-Gingerol	Antiviral (Rhinovirus)	0.553	0.012	High

Compound name	Biological activity	Pa	Pi	Criteria
	Antiviral (Influenza)	0.466	0.029	Low
	Antiprotozoal (Leishmania)	0.401	0.048	Low
Bilobetin	Antiprotozoal (Leishmania)	0.535	0.020	High
	Antimycobacterial	0.525	0.016	High
	Antiviral (Herpes)	0.477	0.013	Low
Xylarioic acid B	Protein synthesis inhibitor	0.797	0.002	High
	Protein 50S ribosomal subunit inhibitor	0.711	0.001	High
	Peptidoglycan glycosyltransferase inhibitor	0.523	0.018	High
Brosimacutin C	Antifungal	0.523	0.027	High
	Antiviral (Rhinovirus)	0.619	0.005	High
	Antiviral (Influenza)	0.462	0.029	Low
Ceriporic acid C	Antiviral (Rhinovirus)	0.606	0.006	High
	Peptidoglycan glycosyltransferase inhibitor	0.470	0.029	Low
	Pediculicide	0.455	0.012	Low
Glycerophospho-N-palmitoyl ethanolamine	Antiprotozoal (Leishmania)	0.640	0.012	High
	Antiviral (Rhinovirus)	0.585	0.008	High
	DNA polymerase I inhibitor	0.475	0.010	Low
Garcinol	Antibacterial	0.621	0.008	High
	Antiprotozoal (Trypanosoma)	0.591	0.009	High
	Antiviral (Rhinovirus)	0.488	0.029	Low
(−)-Desoxygambogenin	Antibacterial	0.621	0.008	High
	Antiprotozoal (Trypanosoma)	0.591	0.009	High
	Antiviral (Rhinovirus)	0.488	0.029	Low
3,4-Dihydroxyphenylacetic acid	Membrane integrity agonist	0.918	0.007	Very high
	Penicillin amidase inhibitor	0.912	0.002	Very high
	Antiseborrheic	0.868	0.007	Very high
32-hydroxy-ent-guttiferone M	Antibacterial	0.630	0.007	High
	Antifungal	0.509	0.029	High
	Antimycoplasmal	0.179	0.068	Very low
Nootkatone	Antiprotozoal (Leishmania)	0.523	0.022	High
	Antifungal	0.346	0.064	Low
	Antibacterial	0.316	0.054	Low
Questiomycin C	Antimycobacterial	0.500	0.019	High
	Antituberculosic	0.284	0.080	Very low
	Antibacterial	0.273	0.071	Very low
(+)-ar-Turmerone	Antifungal	0.557	0.023	High

Compound name	Biological activity	Pa	Pi	Criteria
	Antiviral (Rhinovirus)	0.498	0.025	Low
	Antiparasitic	0.463	0.020	Low
Polygodial	Antifungal	0.444	0.040	Low
	Peptidoglycan glycosyltransferase inhibitor	0.458	0.032	Low
	Antiacne	0.442	0.009	Low
Ginkgetin	Antiprotozoal (Leishmania)	0.544	0.019	High
	Antimycobacterial	0.523	0.016	High
	Antifungal	0.514	0.028	High
Thermolide G	Antifungal	0.887	0.002	Very high
	Antibacterial	0.782	0.003	High
	Antiparasitic	0.682	0.006	High
Caerulomycin F	Antiviral (Picornavirus)	0.532	0.038	High
	Antiprotozoal (Amoeba)	0.525	0.008	High
	Anti-Helicobacter pylori	0.482	0.005	Low
Momilactone	Antifungal	0.467	0.036	Low
	Antiprotozoal (Leishmania)	0.485	0.026	Low
	Antibacterial	0.338	0.046	Low
18-β-Glycyrrhetinic acid	Antiviral (Influenza)	0.892	0.002	Very high
	Antifungal	0.570	0.022	High
	Antibacterial	0.352	0.043	Low
Punctaporonin K	Antiviral (Rhinovirus)	0.471	0.037	Low
	Antibacterial	0.392	0.032	Low
	Antifungal	0.319	0.074	Low
Aqabamycin A	Glucan endo-1,6-beta-glucosidase inhibitor	0.776	0.010	High
	Antiviral (Picornavirus)	0.631	0.013	High
	Antibacterial	0.188	0.130	Low
Farinomalein	Muramoyltetrapeptide carboxypeptidase inhibitor	0.889	0.004	Very high
	Glucan endo-1,3-beta-D-glucosidase inhibitor	0.885	0.003	Very high
	Tpr proteinase (Porphyromonas gingivalis) inhibitor	0.842	0.003	Very high
Malyngolide dimer	Beta-mannosidase inhibitor	0.752	0.004	High
	Glucan endo-1,3-beta-D-glucosidase inhibitor	0.593	0.029	High
	Antiviral (Picornavirus)	0.490	0.055	Low
Pulcherriminic acid	RNA-directed RNA polymerase inhibitor	0.588	0.003	High

Compound name	Biological activity	Pa	Pi	Criteria
	Glucan endo-1,6-beta-glucosidase inhibitor	0.585	0.037	High
	Glucan endo-1,3-beta-D-glucosidase inhibitor	0.453	0.077	Low
Mimosamycin	Antimycobacterial	0.426	0.033	Low
	Antituberculosic	0.413	0.028	Low
	Antibacterial	0.372	0.037	Low
Asperglaucide	Antiviral (Picornavirus)	0.434	0.085	Low
	Antiviral (Adenovirus)	0.296	0.092	Very low
	Antiviral (Poxvirus)	0.232	0.114	Very low
Helquinoline	Antituberculosic	0.274	0.087	Very low
	Isopenicillin-N epimerase inhibitor	0.275	0.089	Very low
	Glucan 1,3-beta-glucosidase inhibitor	0.204	0.014	Very low
5-O-Desosaminyl-6-O-methylerythronolide A	Antiinfective	0.980	0.002	Very high
	Anti-Helicobacter pylori	0.957	0.001	Very high
	Antiprotozoal (Leishmania)	0.953	0.002	Very high
Carbazomycin B	Anti-Helicobacter pylori	0.254	0.058	Very low
	Antiprotozoal (Leishmania)	0.387	0.054	Low
	Antiprotozoal (Trypanosoma)	0.258	0.139	Very low

Prediction of drug-likeness

The analysis revealed varying degrees of compliance with drug-likeness criteria among the compounds derived from *S. junghuhnianum* (**Table 4**). According to Lipinski's Rule of 5, compounds with a molecular weight (MW) ≤ 500 g/mol, logP ≤ 5, no more than 10 hydrogen bond acceptors (N and O atoms), and no more than 5 hydrogen bond donors (NH and OH groups), and with no more than one rule violation tend to exhibit good permeability and absorption in the gastrointestinal tract [23]. Most compounds, such as 4-methoxycinnamaldehyde, 6-gingerol, xylarioic acid B, nootkatone, polygodial, and momilactone, showed no violations, indicating balanced lipophilicity and hydrogen-bonding capacity that support membrane permeability. Recent studies further support these observations, showing that compounds with excessively high logP or MlogP values often face limitations in drug development and require optimization to improve their pharmacokinetic behavior and overall drug-likeness [24,25]. These findings highlight the importance of fine-tuning molecular properties to enhance both efficacy and safety profiles of lead candidates.

Several other compounds, including guttiferone E, ursolic acid, bilobetin, and ginkgetin, exhibited a single Lipinski rule violation, typically related to MW or logP. A single violation is generally considered acceptable, as many bioactive natural products share similar physicochemical characteristics and nevertheless display potent biological activity. In contemporary drug discovery, such molecules remain suitable for further optimization through structural modification or formulation strategies. Conversely, compounds such as malyngolide dimer and 5-O-desosaminyl-6-O-methylerythronolide A showed 2 violations, mainly due to their high molecular weight and excessive numbers of hydrogen bond donors or acceptors. Compounds with more than one violation are more likely to exhibit low membrane permeability and limited oral bioavailability, and therefore may require advanced strategies such as

nanoformulations, prodrug approaches, or targeted delivery systems to improve their pharmacokinetic profiles.

Overall, these results indicate that most metabolites listed in **Table 4** possess physicochemical properties that are compatible with preliminary drug-likeness assessment. Compounds with no Lipinski violations may be prioritized for further exploratory studies, while those with one or more violations remain relevant within a natural-product-oriented discovery framework, particularly considering that many bioactive natural compounds fall within the "beyond the rule of five" (bRO5) chemical space.

Table 4 Physicochemical properties of compounds from *Sphagnum junghuhnianum* based on Lipinski's Rule of 5.

Compound name	Lipinski				
	MW	**MlogP ≤ 4.15**	**NorO ≤ 10**	**NHorOH ≤ 5**	**Violation**
4-(3-Dodecanyl)Benzenesulfonic Acid	326.49	4.49	3	1	Yes (1)
Gluconic Acid	196.16	–2.90	7	6	Yes (1)
4-Methoxycinnamaldehyde	162.19	1.66	2	0	Yes (0)
Guttiferone E	602.80	3.78	10	6	Yes (1)
Ursolic Acid	456.70	5.82	3	2	Yes (1)
6-Gingerol	294.39	2.14	4	2	Yes (0)
Bilobetin	552.48	0.44	10	5	Yes (1)
Xylarioic acid B	234.29	0.31	5	4	Yes (0)
Brosimacutin C	342.39	1.63	5	3	Yes (0)
(−)-Desoxygambogenin	600.78	4.12	6	2	Yes (1)
3,4-Dihydroxyphenylacetic acid	168.15	0.47	4	3	Yes (0)
32-hydroxy-ent-guttiferone M	618.80	2.98	7	4	Yes (1)
Nootkatone	218.33	3.46	1	0	Yes (0)
Questiomycin C	274.30	–0.00	4	1	Yes (0)
(+)-ar-Turmerone	216.32	3.68	1	0	Yes (0)
Polygodial	234.33	2.54	2	0	Yes (0)
Ginkgetin	566.51	0.63	10	4	Yes (1)
Thermolide G	629.87	2.06	9	5	Yes (1)
Caerulomycin F	216.24	0.02	4	1	Yes (0)
Momilactone	314.42	3.57	3	0	Yes (0)
18-β-Glycyrrhetinic acid	470.68	4.87	4	2	Yes (1)
Aqabamycin A	265.26	2.05	3	2	Yes (0)
Farinomalein	211.21	0.55	4	1	Yes (0)
Malyngolide dimer	540.82	4.52	6	2	No (2)
Mimosamycin	233.22	–0.34	4	0	Yes (0)
Asperglaucide	444.52	3.41	4	2	Yes (0)
5-O-Desosaminyl-6-O-methylerythronolide A	589.76	–0.16	11	4	No (2)
Carbazomycin B	241.29	2.35	2	2	Yes (0)

Notes: MW: Molecular Weight (measured in g/mol); MlogP: Calculated octanol/water partition coefficient (lipophilicity); NorO: Total oxygen atoms; NhorOH: Total nitrogen + hydroxyl groups.

Molecular interactions of *Sphagnum junghuhnianum* bioactive compounds with PBP1 (7O4B)

Molecular docking analysis was conducted using Penicillin-Binding Protein 1 (PBP1; PDB ID: 7O4B), a transpeptidase involved in peptidoglycan biosynthesis in *Staphylococcus aureus*. The docking results (**Table 5**) demonstrated variation in predicted binding energies, ranging from −5.7 to −9.8 kcal/mol, suggesting differential ligand accommodation within the PBP1 active-site region. Among the analyzed compounds, ursolic acid showed the most favorable binding affinity (−9.8 kcal/mol), exceeding that of the reference inhibitor (7OPB; −7.3 kcal/mol).

Ursolic acid was predicted to interact predominantly through hydrophobic contacts with residues ILE348, LEU416, PHE423, TYR527, and TYR534, along with a π-sigma interaction involving TYR534. These interactions suggest that the triterpenoid scaffold of ursolic acid may fit favorably within a hydrophobic region of the PBP1 binding pocket. Other compounds with comparatively low binding energy values included bilobetin and thermolide G (both −9.4 kcal/mol), which formed multiple predicted hydrogen bonds with residues such as SER349, ARG353, SER368, THR514, THR516, and TYR534 (**Figures 4** and **5**). The presence of hydroxyl and phenolic functional groups in these molecules may contribute to their predicted interaction patterns.

Additional metabolites, including 18-β-glycyrrhetinic acid, brosimacutin C, nootkatone, and (−)-desoxygambogenin, were also predicted to interact with residues frequently associated with the PBP1 binding site, such as SER314, SER368, ASN370, THR514/516, TRP351, PHE423, TYR534, and TYR566. The recurrence of these interactions across multiple ligands suggests a degree of structural compatibility with the PBP1 active-site environment.

Overall, the docking results indicate that hydrogen bonding involving polar residues (e.g., SER, THR, ASN) and hydrophobic or aromatic interactions involving residues such as TRP, PHE, and TYR may contribute to ligand stabilization within the PBP1 binding region. However, these interaction patterns should be interpreted as computational predictions that provide preliminary, hypothesis-generating insights, rather than direct evidence of enzymatic inhibition or disruption of peptidoglycan biosynthesis. Experimental validation through quantitative enzymatic or cellular assays will be necessary to clarify the functional relevance of these predicted interactions.

Table 5 Binding residues and binding energies of bioactive compounds from *Sphagnum Junghuhnianum* docked with 7O4B (Pbp1).

Ligand	Interaction with				Binding Affinity (kcal/mol)
	Conventional H-Bond	Carbon H-Bond	Pi-Alkyl	Pi-Sigma	
Control (7OPB)	SER A:314 SER A:368 ASN A:370 GLN A:425 THR A:516		TYR A:566	TRP A:351	–7.3
Bioactive components of the *S. junghuhnianum*					
4-(3-Dodecanyl) Benzenesulfonic Acid	SER A:314 ASN A:370		HIS A:499	TRP A:351	–6.9

Ligand	Interaction with				Binding Affinity (kcal/mol)
	Conventional H-Bond	Carbon H-Bond	Pi-Alkyl	Pi-Sigma	
Gluconic Acid	SER A:314 SER A:368 ASN A:370 THR A:516	TRP A:351			–5.7
4-Methoxycinnamaldehyde	SER A:314 SER A:368 LYS A:317				–5.7
Guttiferone E	SER A:314 ASN A:370		ILE A:348 PHE A:423 PRO A:533	TYR A:566	–8.2
Ursolic Acid			ILE A:348 LEU A:416 PHE A:423 TYR A:527	TYR A:534	–9.8
6-Gingerol	SER A:314 SER A:368 ASN A:370 TYR A:534	THR A:514	PHE A:423		–6.1
Bilobetin	SER A:349 ARG A:353 SER A:368 THR A:514	THR A:516 TYR A:534			–9.4
Xylarioic acid B	TYR A:503 THR A:516 GLY A:515 SER A:537	GLY A:569	TYR A:566	TRP A:351	–6.5
Brosimacutin C	SER A:314 LYS A:317 SER A:368 TYR A:534				–8.2
(−)-Desoxygambogenin	SER A:314 ASN A:370 TYR A:534		LYS A:529 PRO A:533 TYR A:566		–7.8
3,4-Dihydroxyphenylacetic acid	ARG A:353 ASN A:370 TYR A:534		TYR A:566		–7.9

Ligand	Interaction with				Binding Affinity (kcal/mol)
	Conventional H-Bond	Carbon H-Bond	Pi-Alkyl	Pi-Sigma	
32-hydroxy-ent-guttiferone M	SER A:314 ASN A:370 THR A:514 THR A:516				–6.1
Nootkatone	SER A:349		ILE A:348 TRP A:351 PHE A:423 TYR A:527 TYR A:566		–8.1
Questiomycin C	THR A:514			TRP A:351 TYR A:566	–6.9
(+)-ar-Turmerone	SER A:314 THR A:516 TYR A:566				–7.9
Polygodial	SER A:314 LYS A:317 SER A:368		HIS A:499	TRP A:351	–6.8
Ginkgetin	SER A:314 LYS A:317 SER A:368		TYR A:534 TYR A:566		–6.9
Thermolide G	SER A:349 ARG A:353 SER A:368 THR A:514	THR A:516 TYR A:534 TYR A:566			–9.4
Caerulomycin F	SER A:314 LYS A:317 SER A:349 SER A:368 THR A:514	ALA A:500	TRP A:351 PHE A:423 TYR A:534 TYR A:566		–8.1
Momilactone	TRP A:351 THR A:516				–6.9
18-β-Glycyrrhetinic acid	THR A:514 THR A:516		TRP A:351 ALA A:500 TYR A:566		–8.7

Ligand	Interaction with				Binding Affinity (kcal/mol)
	Conventional H-Bond	Carbon H-Bond	Pi-Alkyl	Pi-Sigma	
Aqabamycin A	SER A:314 SER A:368 THR A:514 THR A:516 TYR A:566		TRP A:351		–7.6
Farinomalein	THR A:514				–7.8
Mimosamycin	SER A:314 SER A:368 TYR A:566		PHE A:423	TRP A:351	–6.5
Helquinoline	SER A:314 SER A:368 LYS A:317 ASN A:370 TYR A:566	PHE A:423 THR A:516		TRP A:351	–7.4
Carbazomycin B	TYR A:503 THR A:514 GLY A:515 THR A:516 SER A:537		ALA A:500		–7.4

The *in-silico* analyses were evaluated in relation to the *in vitro* antimicrobial screening results presented in **Table 1**. The methanolic extract of *S. junghuhnianum* exhibited concentration-dependent antibacterial effects in disk diffusion assays, with the largest inhibition zones observed at 100% extract concentration, particularly against *S. pyogenes* (42.01 ± 0.33 mm) and *S. aureus* (34.62 ± 2.21 mm). These Gram-positive pathogens rely on penicillin-binding proteins (PBPs) for cell wall biosynthesis, which may partly explain their higher susceptibility under the tested conditions. Moderate inhibition was also observed against *S. typhi* (22.36 ± 0.84 mm) and *P. gingivalis* (18.05 ± 0.41 mm), whereas no inhibition was detected against *K. pneumoniae* or *A. niger*, indicating a selective antibacterial spectrum of the extract.

Consistent with the antibacterial screening results, the extract did not exhibit antifungal activity against *C. albicans*, as no inhibition zone was observed, while the positive control produced clear antifungal effects. Molecular docking analysis suggested that several moss-derived metabolites may interact favorably with the PBP1 active site, exhibiting binding poses and affinity values comparable to or lower than those of the reference ligand. These predicted interactions provide preliminary insights into a possible molecular basis for the preferential antibacterial activity observed against Gram-positive bacteria. However, such interactions should be regarded as hypothesis-generating, as molecular docking alone does not confirm enzymatic inhibition or downstream effects on peptidoglycan biosynthesis.

Overall, this study indicates that *S. junghuhnianum* is a chemically rich source of secondary metabolites with potential antibacterial relevance. LC-HRMS profiling revealed 514 putatively identified metabolites, of which 35 compounds were selected for further computational evaluation based on database

annotation and PASS predictions. By integrating *in vitro* antibacterial screening with metabolomic profiling and *in silico* analyses, this work provides preliminary, multi-level evidence supporting the antibacterial potential of *S. junghuhnianum* metabolites. Further studies involving quantitative antimicrobial assays, compound isolation, and target-based validation are required before their potential application in antimicrobial drug development can be fully assessed.

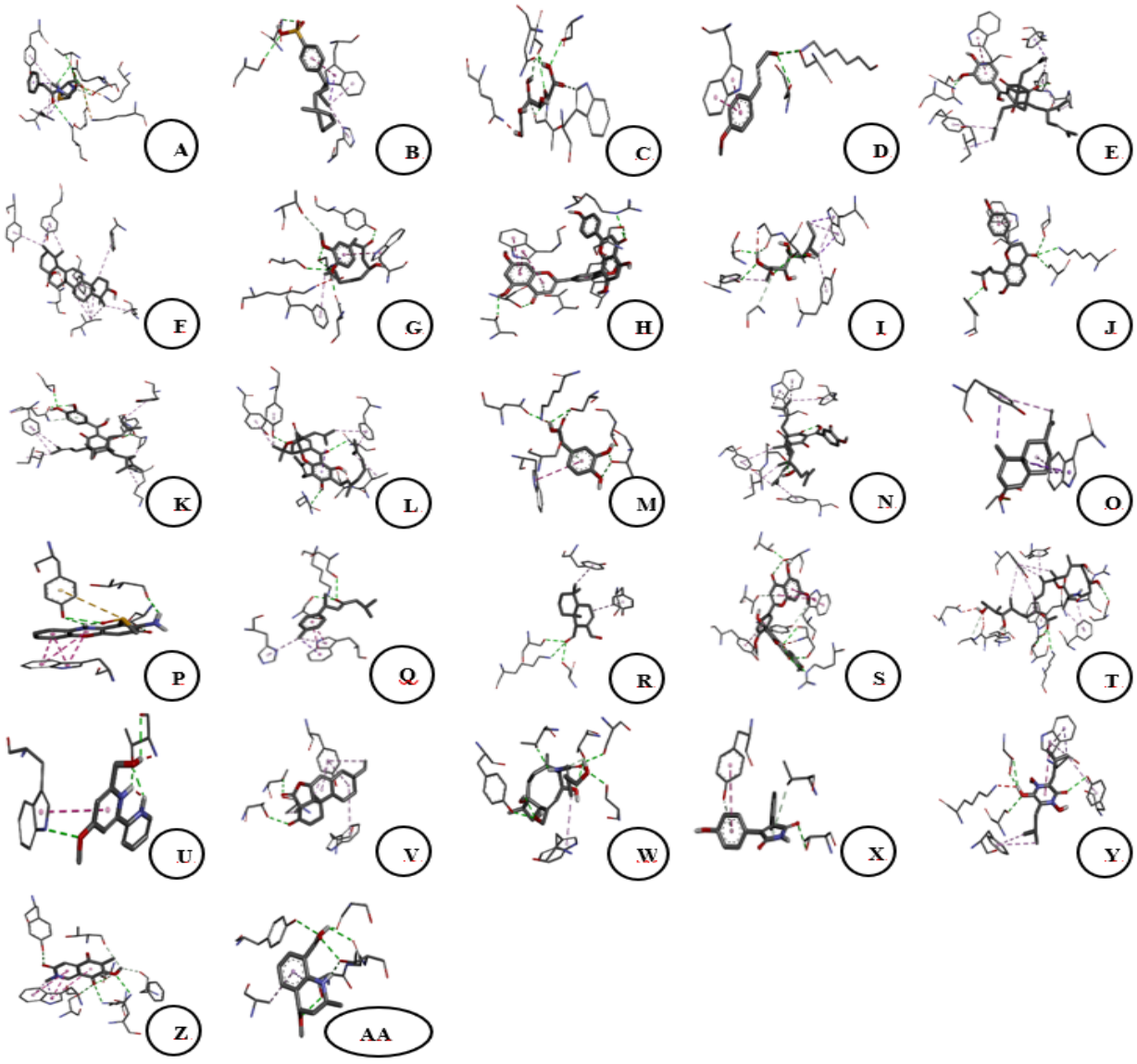

Figure 4 Three-dimensional binding interactions of 7OPB (control) and bioactive compounds from *Sphagnum junghuhnianum* with the 7O4B protein (PBP1). A. 7OPB; B. 4-(3-Dodecanyl) Benzenesulfonic Acid; C. Gluconic Acid; D. 4-Methoxycinnamaldehyde; E. Guttiferone E; F. Ursolic Acid; G. 6-Gingerol; H. Bilobetin; I. Xylarioic acid B; J. Brosimacutin C; K. (−)-Desoxygambogenin; L. 3,4-Dihydroxyphenylacetic acid; M. 32-hydroxy-ent-guttiferone N; L. Nootkatone; O. Questiomycin P; N. (+)-ar-Turmerone; Q. Polygodial; R. Ginkgetin; S. Thermolide G; T. Caerulomycin U; S. Momilactone; V. 18-β-Glycyrrhetinic acid; W. Aqabamycin A; X. Farinomalein; Y. Mimosamycin; Z. Helquinoline; AA. Carbazomycin B.

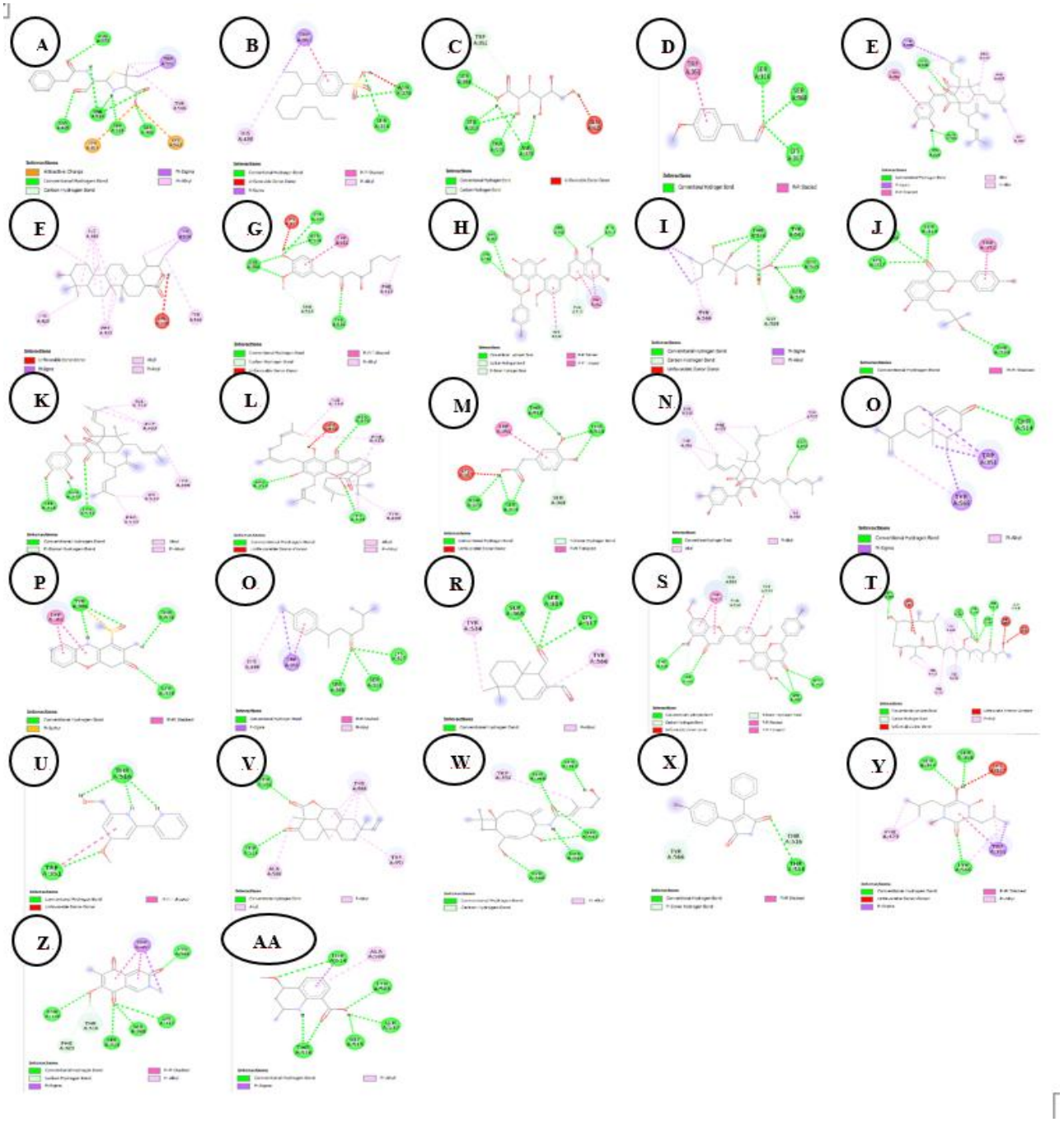

Figure 5 Two-dimensional binding interactions of 7OPB (control) and bioactive compounds from Sphagnum junghuhnianum against the 7O4B protein. A. 7OPB; B. 4-(3-Dodecanyl) Benzenesulfonic Acid; C. Gluconic Acid; D. 4-Methoxycinnamaldehyde; E. Guttiferone E; F. Ursolic Acid; G. 6-Gingerol; H. Bilobetin; I. Xylarioic acid B; J. Brosimacutin C; K. (−)-Desoxygambogenin; L. 3,4-Dihydroxyphenylacetic acid; M. 32-hydroxy-ent-guttiferone N; L. Nootkatone; O. Questiomycin P; N. (+)-ar-Turmerone; Q. Polygodial; R. Ginkgetin; S. Thermolide G; T. Caerulomycin U; S. Momilactone; V. 18-β-Glycyrrhetinic acid; W. Aqabamycin A; X. Farinomalein; Y. Mimosamycin; Z. Helquinoline; AA. Carbazomycin B.

Conclusions

The methanolic extract of *Sphagnum junghuhnianum* demonstrated notable antibacterial activity in preliminary disk diffusion assays, particularly against Gram-positive bacteria, while no antifungal activity was observed under the tested conditions. LC-HRMS profiling revealed a chemically diverse metabolite composition, with several compounds putatively identified as having potential antimicrobial relevance. *In silico* molecular docking analysis suggested favorable interactions of ursolic acid, bilobetin, and thermolide G with Penicillin-Binding Protein 1 (PBP1), providing preliminary insights into a possible antibacterial mode of action. Overall, these findings indicate that *S. junghuhnianum* represents a promising source of antibacterial candidates, warranting further studies involving quantitative antimicrobial assays, compound isolation, and experimental validation to support its potential for future drug development.

Acknowledgements

This research was supported by the Ministry of Education, Culture, Research and Technology of the Republic of Indonesia, through the BIMA Research Grant (Contract Number: 112/C3/DT.05.00/PL/2025).

Declaration of Generative AI in Scientific Writing

The authors acknowledge the use of generative AI tools (such as QuillBot and ChatGPT by OpenAI) in thepreparation of this manuscript, specifically for language editing and grammar correction. No content generation or data interpretation was performed by AI. The authors take full responsibility for the content and conclusions of this work.

CRediT author statement

Sinta R Pardosi: Investigation, methodology, data collection, data analysis, original draft writing. **Etti Sartina Siregar**: Conceptualization, investigation, review, editing, corresponding author. **Isnaini Nurwahyuni**: Research design, project administration, data curation, review, editing.

References

[1] GV Naumova, AE Tomson, NA Zhmakova, NL Makarova and TF Ovchinnikova. Biologically active compounds of different sphagnum peat species. *Solid Fuel Chemistry* 2015; **49**, 135-140.

[2] F Chen, A Ludwiczuk, G Wei, X Chen, B Crandall-Stotler and JL Bowman. Terpenoid secondary metabolites in bryophytes: Chemical diversity, biosynthesis and biological functions. *Critical Reviews in Plant Sciences* 2018; **37(2-3)**, 210-231.

[3] G Montenegro, MC Portaluppi, FA Salas and MF Díaz. Biological properties of the chilean native moss *Sphagnum magellanicum*. *Biological Research* 2009; **42(2)**, 233-237.

[4] D Stenitzer, R Mócsai, H Zechmeister, R Reski, EL Decker and F Altmann. *O*-methylated N-glycans distinguish mosses from vascular plants. *Biomolecules* 2022; **12(1)**, 136.

[5] M Hymas, I Casademont-Reig, S Poigny and VG Stavros. Characteristic photoprotective molecules from the sphagnum world: A solution-phase ultrafast study of sphagnic acid. *Molecules* 2023; **28(16)**, 6153.

[6] JD Fudyma, J Lyon, R AminiTabrizi, H Gieschen, RK Chu, DW Hoyt, JE Kyle, J Toyoda, N Tolic, HM Heyman, NJ Hess, TO Metz and MM Tfaily. Untargeted metabolomic profiling of *Sphagnum fallax* reveals novel antimicrobial metabolites. *Plant Direct* 2019; **3(10)**, e00179.

[7] L Bryan, R Shaw, E Schoonover, A Koehl, S DeVries-Zimmerman and M Philben. Sphagnan in Sphagnum-dominated peatlands: Bioavailability and effects on organic matter stabilization. *Biogeochemistry* 2024; **167**, 665-680.

[8] RS Shete, HV Wangikar, JJ Chavan, MB Kanade and SJ Chavan. Bioactive compounds of bryophytes: Unveiling antimicrobial properties and therapeutic potential. *International Journal of Plant and Environment* 2024, **10(3)**, 1-15.

[9] TA Çelik, ÖS Aslantürk, G Aslan and M Kirmaci. Determination of phytochemical content and antioxidant activities of *Sphagnum divinum* Flatberg & K. Hassel and *Sphagnum girgensohnii*

Russow (Sphagnopsida). *Anatolian Bryology* 2022; **9(2)**, 58-69.

[10] M Singh, AKS Rawat and R Govindarajan. Antimicrobial activity of some Indian mosses. *Fitoterapia* 2007; **78(2)**, 156-158.

[11] DR Chhetri, S Yonzone and R Mukhia. Bioprospecting for enzymes in bryophytes: Extraction of L-Myo-inositol-1-phosphate synthase from Sphagnum junghuhnianum Doz. et Molk. and its characterization. *South African Journal of Botany* 2023; **136**, 692-702.

[12] K Wacnik, VA Rao, X Chen, L Lafage, M Pazos, S Booth, W Vollmer, JK Hobbs, RJ Lewis and SJ Foster. Penicillin-binding protein 1 (PBP1) of *Staphylococcus aureus* has multiple essential functions in cell division. *mBio* 2022; **13(4)**, 0066922.

[13] DPM Sethuvel, YD Bakthavatchalam, MKM Irulappan, R Sherivastava, H Periasamy and V Veeraghavan. β-Lactam resistance in ESKAPE pathogens mediated through modifications in penicillin-binding proteins: An overview. *Infectious Diseases and Therapy* 2023; **12**, 829-841.

[14] S Martinez-Caballero, KV Mahasenan, C Kim, R Molina, R Feltzer, M Lee, R Bouley, D Hesek, JF Fisher, IG Muñoz, M Chang, S Mobashery and JA Hermoso. Integrative structural biology of the penicillin-binding protein-1 from *Staphylococcus aureus*, an essential component of the divisome machinery. *Computational and Structural Biotechnology Journal* 2021; **19**, 5392-5405.

[15] L Wu, Y Zhang, J Yang, H Liu and S Wang. Diversity and correlation analysis of microbiomes and metabolites of *Sphagnum palustre* in various microhabitats. *BMC Plant Biology* 2025; **25**, 761.

[16] J Hudzicki. Kirby-Bauer disk diffusion susceptibility test protocol. *ASM* 2019; **15(1)**, 1-23.

[17] LR Valeeva, AL Dague, MH Hall, AE Tikhonova, MR Sharipova, MA Valentovic, LM Bogomolnaya and EV Shakirov. Antimicrobial activities of secondary metabolites from moss: A review. *Antibiotics* 2022; **11**, 1004.

[18] L Klavina, G Springe, V Nikolajeva, I Martsinkevich, I Nakurte, D Dzabijeva and I Steinberga Chemical composition analysis, antimicrobial activity and cytotoxicity screening of moss extracts (Moss phytochemistry). *Molecules* 2015; **20(9)**, 17221-17243.

[19] S Xu, Y Li, H Wang, J Chen, L Liu and F Zhao. Plant flavonoids with antimicrobial activity against methicillin-resistant *Staphylococcus aureus* (MRSA). *ACS Infectious Diseases* 2024; **10(8)**, 1594-1612.

[20] L Krunova, L Valeeva, A Ivanova, D Petrova, S Smirnov and E Fedorova. Antimicrobial activities of secondary metabolites from model mosses. *Antibiotics* 2022; **11(8)**, 1004.

[21] ML Astolfi, A Bianchi, F Rossi, G Conti, L Marino, P Santini and R De Luca. Sphagnum moss and peat comparative study: Metal release, binding properties and antioxidant activity. *PLoS One* 2024; **19(8)**, e0307210.

[22] A Lagunin, A Stepanchikova, D Filimonov and V Poroikov. PASS: prediction of activity spectra for biologically active substances. *Bioinformatics* 2000; **16(8)**, 747-748.

[23] CA Lipinski, F Lombardo, BW Dominy and PJ Feeney. Experimental and computational approaches to estimate solubility and permeability in drug discovery and development settings. *Advanced Drug Delivery Reviews* 1997; **23(1-3)**, 3-25.

[24] V Ivanović, M Rančić, B Arsić and A Pavlović. Lipinski's rule of five, famous extensions and famous exceptions. *Chemia Naissensis* 2020; **3(1)**, 171-177.

[25] TK Karami, S Hailu, S Feng, R Graham and HJ Gukasyan. Eyes on Lipinski's rule of five: A new “rule of thumb” for physicochemical design space of ophthalmic drugs. *Journal of Ocular Pharmacology and Therapeutics* 2022; **38(1)**, 43-55.